Acta Crystallographica Section B
Structural Science
ISSN 0108-7681

Invariom modeling of ceftazidime pentahydrate: molecular properties from a 200 second synchrotron microcrystal experiment

C. J. Schürmann,[a] K. Pröpper,[a] T. Wagner[b] and B. Dittrich[a]*

[a]Institut für Anorganische Chemie der Universität Göttingen, Tammannstr. 4, Göttingen D-37077, Germany, and [b]Analytical Sciences, Novartis Institutes for BioMedical Research, WSJ-503.12.02, Basel CH-4002, Switzerland

Correspondence e-mail: bdittri@gwdg.de

Received 9 November 2011
Accepted 21 April 2012

© 2012 International Union of Crystallography
Printed in Singapore – all rights reserved

The structure of ceftazidime pentahydrate, a third generation cephalosporin antibiotic, is reported. Data collection was carried out in a remarkably short time with synchrotron radiation and the latest detector technology, illustrating that single-crystal X-ray diffraction can be used as a technique for screening hundreds of compounds in a short amount of time. Structure refinement made use of invariom, namely non-spherical scattering factors, which allow more information to be derived from a diffraction experiment. Properties that can be screened are bond-topological parameters, empirical hydrogen-bond energies, molecular dipole moments and electrostatic potentials.

1. Introduction

Cephalosporins are among the most frequently used broad-spectrum antimicrobial agents. Cefdinir is currently the best-selling drug of this class. The mechanism of action of their antibacterial activity is analogous to penicillins in that molecules interfere with the bacterial cell-wall synthesis of penicillin-binding proteins (PBPs). Concerning the question of resistance the structure of a class C β-lactamase in a complex with ceftazidime was elucidated (Powers *et al.*, 2001). Single-crystal X-ray structures of cephalosporins are commonly of low quality, probably due to disorder caused by the conformational flexibility of the cephem ring structure or a lack of matching intermolecular interactions. The tendency of several cephalosporins to form solvates, co-crystals and channel structures (Kemperman *et al.*, 1999, 2000, 2001; Stephenson & Diseroad, 2000; Kennedy *et al.*, 2003) is probably also related to the flexibility of the cephem ring. Consequently, several cephalosporin structures remain unknown, and despite the importance of cephalosporins in the market not many structures have been determined to a high accuracy. Ceftazidime, a semisynthetic β-lactam antibiotic for parenteral administration, has been categorized as a third-generation cephalosporin antibiotic according to the range of antibacterial specificity of these molecules. The absolute structure and molecular conformation in the solid state have so far not been characterized by single-crystal X-ray diffraction. We here report the structure of the pentahydrate of ceftazidime, the marketed form, and confirm the absolute configuration of the chiral centers.

We were only able to obtain microcrystals for ceftazidime. For structure solution from such small specimens the abundance of primary beam intensity at the synchrotron is indispensable to reach the resolution required.

Starting from the the mid 1990s (Koritsanszky *et al.*, 1998; Macchi *et al.*, 1998; Iversen *et al.*, 1999) the advance of area detectors has been a major driving force of progress in single-crystal diffraction. This led to a decrease in data-collection time both at home sources and synchrotrons. Earlier claims on the possibility of high-accuracy single-crystal X-ray diffraction becoming a high throughput screening technique (Luger *et al.*, 2005; Luger, 2007) are currently being substantiated with the advance of a new generation of detectors with even faster read-out times. However, fast data acquisition alone does not allow high-throughput since the time required for data evaluation needs to be taken into account. Only the combination of fast data collection with automated aspherical-atom modeling broadens the applicability for drug design and modeling. Crystalline compounds

Table 1
Crystal and structure refinement data for ceftazidime pentahydrate.

Coordinates of H atoms were set to calculated positions using bond distances obtained from model compounds from the invariom database. Distances to H atoms in the IAM refinement were not elongated.

Crystal data		
Chemical formula	$C_{22}H_{22}N_6O_7S\ _2{\cdot}5H_2O$	
M_r	636.68	
Crystal system, space group	Orthorhombic, $P2_12_12_1$ (No. 19)	
Temperature (K)	100	
a, b, c (Å)	8.9716 (5), 10.3943 (7), 31.5444 (12)	
V (Å^3)	2941.6 (3)	
Z	4	
D_x (Mg m^{-3})	1.438	
Radiation type	Monochromated synchrotron, λ = 0.65000 Å	
μ (mm^{-1})	0.196	
Crystal size (mm)	0.01 × 0.01 × 0.003	
Data collection		
Diffractometer	High-resolution diffractometer with Pilatus 6M	
Absorption correction	Empirical	
T_{min}, T_{max}	0.647, 0.746	
θ_{max} (°)	27.66	
R_{int}†	0.078	
No. of measured, independent and observed [$F > 4\sigma(F)$] reflections	22 933, 8486, 6506	
$(\sin\theta/\lambda)_{max}$ (Å^{-1})	0.714	
Overall completeness (%)	95.2	
Redundancy	4.26	
Refinement		
Number of parameters	380	
Weighting scheme	Based on measured s.u.s‡	
	INV	IAM
N_{ref}/N_{var}	17.12	
$R_1(F)$	0.060	0.062
$wR(F)$	0.067	0.070
S†	1.32	1.37
Flack (1983) parameter	0.01 (11)	0.03 (12)
$\Delta\rho_{max}$, $\Delta\rho_{min}$ (e Å^{-3})	0.54, −0.58	0.52, −0.61

† $R_{int}(F^2) = \sum|F_o^2 - F_o^2(\text{mean})|/\sum F_o^2$. ‡ $w = 1/\sigma^2$, $wR = \{\sum[|w|F_o| - F_c|^2|]/\sum|wF_o^2|\}^{1/2}$, $R_1(F) = \sum||F_o| - |F_c||/\sum|F_o|$, $S = [\sum||F_o| - k|F_c||^2)/(n_o - m_{var})]^{1/2}$.

where scattering power is not sufficient to meet the requirements of a charge-density study (amongst other criteria low-temperature data collection, $\sin\theta/\lambda \geq 1.0$Å^{-1}) can be rapidly investigated this way (Hübschle *et al.*, 2007).

2. Experimental, structure solution and initial refinement

Ceftazidime was purchased from Sigma–Aldrich and crystallized from water. The single-crystal diffraction experiment was carried out in the remarkably short measurement time of 3 min 20 s at the third-generation synchrotron Swiss Light Source (SLS) at the Paul Scherrer Institute in Switzerland. The crystal was mounted on a commercial 50 µm MiTeGen MicroLoop in Paratone N mounting oil and discarded after the measurement. The beamline used (X10SA) has recently been equipped with a new generation of area detectors (the DECTRIS Pilatus 6M detector) that allow shutterless photon detection (Broennimann *et al.*, 2006). While the detector design allows a continuous readout (Bronnimann *et al.*, 2003), individual frames with a fine φ-slicing of 0.1° were generated for integration with the *XDS* software (Kabsch, 2010) using a standard data collection protocol at the beamline. 1440 frames were collected and the sample–detector distance was 165 mm, which is the minimal distance possible with default beamline settings. The beam size was 50 × 150 µm and the wavelength was chosen to be 0.6500 Å. *XDS* output was converted with the utility program *XDS2SAD* and subsequently processed with *SADABS* (Sheldrick, 2008*b*) performing an empirical absorption correction. Redundant Bragg data – cut at and complete to 0.7 Å^{-1} – were obtained.

The minimum and maximum transmission are rather dissimilar. It is likely that beam fluctuation or imperfect centering of the sample have also been taken into account by the multiscan (Blessing, 1995) procedure. The small sample size required full intensity to reach the comparably high resolution. The unattenuated beam led to detector saturation of some low-order reflections and a rather high internal R factor. The likelihood of detector oversaturation is reduced for the Pilatus detector, since the dynamic range increases from 16 bit (common CCDs) to 20 bit (Pilatus). However, detector oversaturation for the Pilatus is not immediately visible on the frames from 'bleeding' anymore (like it used to be for CCD detectors) and needs to be checked from the integration output. The absence of these oversaturated low-order reflections reduces the signal for bonding electron density. Attempts to improve the counting statistics by varying measurement time and filters did not lead to better data quality, maybe because radiation damage already affected the crystal quality. Past and recent (Toyokawa *et al.*, 2010) systematic studies aiming for better data quality using these detectors will hopefully help to obtain the best possible data routinely. Nevertheless, considering the small size of the specimen, comparably good data were obtained in a remarkably short time.

Structure solution and initial independent atom model (IAM) least-squares refinement was performed with *SHELXS* and *SHELXL* (Sheldrick, 2008*a*) interfaced to the graphical user interface *SHELXLE* (Hübschle *et al.*, 2011).

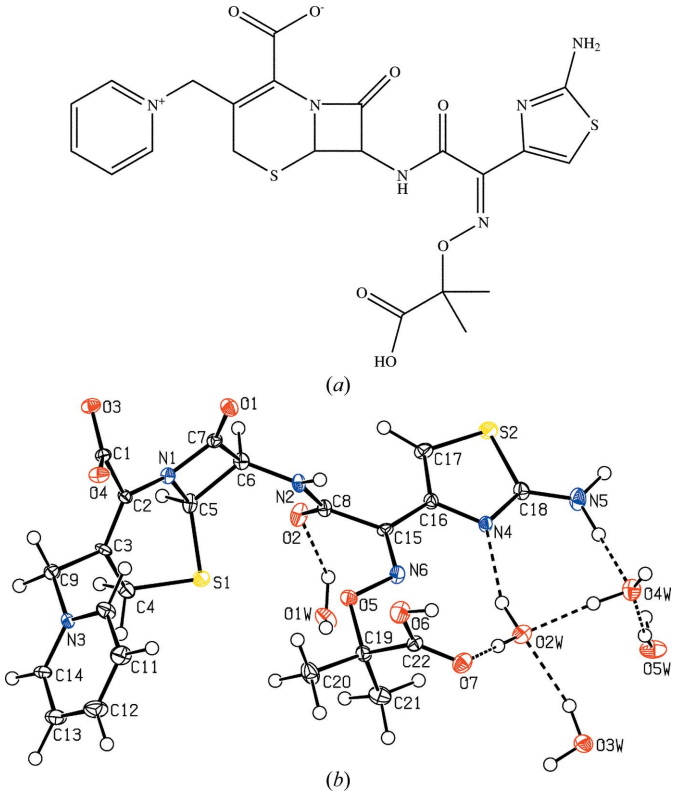

Figure 1
(*a*) Schematic diagram of ceftazidime and (*b*) *ORTEP* representation (Burnett & Johnson, 1996) of the experimentally determined asymmetric unit structure in the crystal with atom-numbering scheme (bottom). The plot was generated by the program *PLATON* (Spek, 2009); ellipsoids are at 50% probability.

Fig. 1 shows the molecular structure and its *ORTEP* (Burnett & Johnson, 1996) representation after invariom refinement (INV, see §2.1) as generated by the program *PLATON* (Spek, 2009). Full crystallographic details are given in Table 1 and the supplementary information.[1]

2.1. Invariom refinement

Whereas in 1998 (Koritsanszky *et al.*, 1998) rapid data collection with CCD detectors compared with scintillation counters was a major technical advance, the further order of magnitude gained in data acquisition time due to recent detector development can only fully be exploited by simultaneously speeding up the data evaluation process. This is now possible by earlier (Dittrich *et al.*, 2004, 2005; Dittrich, Hübschle *et al.*, 2006) and ongoing improvements in invariom modeling as based on the Hansen–Coppens multipole model (Hansen & Coppens, 1978). Details on these improvements will be published in a forthcoming paper. In principle, the two other scattering factor databases (Zarychta *et al.*, 2007; Dominiak *et al.*, 2007) likewise would enable rapid data evaluation. However, the invariom database offers – with over 1900 scattering factors and growing – the largest variety of chemical environments. For ceftazidime pentahydrate the electron density was reconstructed from 34 geometry-optimized model compounds using 44 different invariom scattering factors, as listed in the supplementary material.

Today, continuous efforts in software development allow a routine and user-friedly application of the invariom approach. In recent software updates the functionality for a riding hydrogen treatment was added. Hydrogen constraints can now be generated for the *XD* program-suite system files (Koritsánszky *et al.*, 2003; Volkov *et al.*, 2006) by utilizing the preprocessor program *InvariomTool* (Hübschle *et al.*, 2007), which was used to set up *XD* system files for ceftazidime. In this step, U_{iso} of riding H atoms were also constrained to a factor of 1.2 (C_{arom}, CH, NH, CH_2) or 1.5 (CH_3, H_2O) of the respective non-H atom. For the title compound such a constrained refinement was combined with setting the bond distances to H atoms to values obtained from the invariom database in order to give the best fit to the diffraction data. Despite the capability to automate scattering-factor assignment with *InvariomTool*, visual inspection of the local atomic coordinate systems is advisable. This holds especially for disordered structures, and this task is greatly facilitated by the visualizer *molecoolQt* (Hübschle & Dittrich, 2011), which now allows the generation of a representation of deformation electron density by a single mouse click from a multipole minus IAM Fourier map. Possible ambiguities in assignment of local-atomic coordinate systems can be spotted immediatedly from such three-dimensional Fourier maps (see Fig. 2*a*). The residual electron density can likewise be displayed in a similar manner.

For chemical environments and functional groups common to organic chemistry the time required to perform an invariom refinement is now comparable to IAM refinement.

3. Results and discussion

Apart from the topological properties of covalent and hydrogen bonds (Bader, 1990) and empirical energetic estimates of hydrogen bonding (Espinosa *et al.*, 1998), further outcomes of studies using the Hansen/Coppens multipole model are improvements in parameter precision and accuracy (Coppens *et al.*, 1969). Here we want to emphasize the reduction of the standard deviation of the Flack (1983) parameter, which is 0.03 (12) after IAM and 0.01 (11) after invariom refinement. Hence the absolute structure of the title compound can be established. A locally modified version of *XDLSM* (Dittrich, Strumpel *et al.*, 2006) was used for Flack-parameter refinement. The noisy low-order data and the dominant core-scattering contribution of the S atoms limit the reduction in the R_1 factor to 0.2% in the case of the title structure. After invariom refinement an improvement in the physical significance of ADPs is also seen: the average of the differences of the mean-square displacement amplitudes in bond direction (Hirshfeld, 1976), which is supposed to be zero for atoms of comparable mass, is reduced from 24×10^{-4} (IAM refinement) to 19×10^{-4}. Such improvements are routine outcomes from invariom modeling.

The electron density model from summation of the invariom fragments furthermore allows the calculation of molecular dipole moments (Spackman, 1992; Spackman *et al.*, 2007) and of the molecular electrostatic potential (Su & Coppens, 1992). It should be noted that crystal-field effects are not taken into account by current theoretical pseudoatom scattering-factor databases. Hence, properties

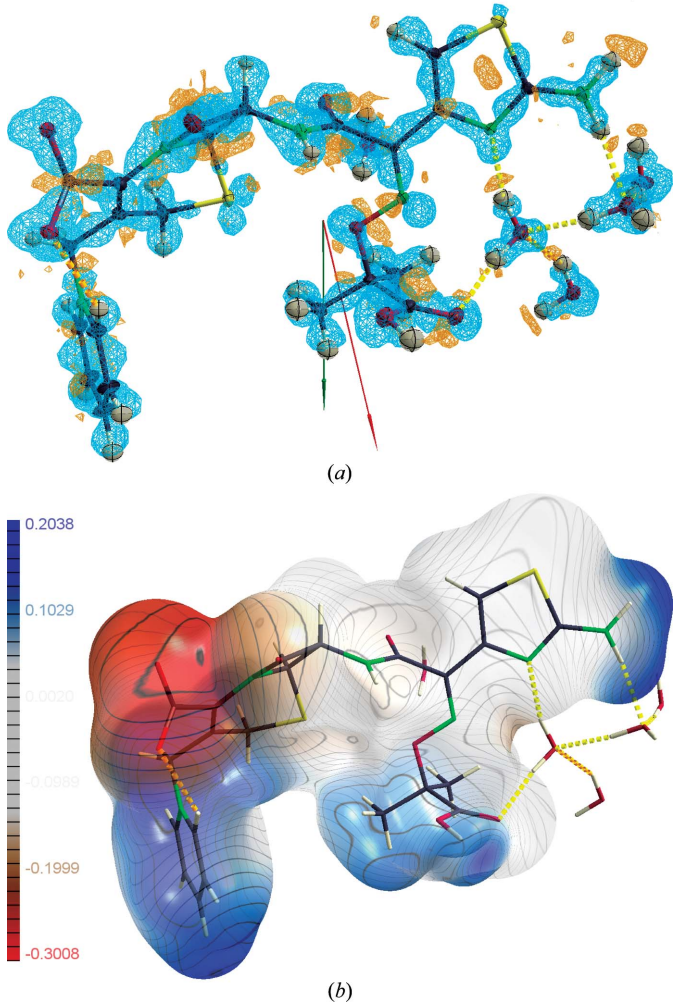

(*a*)

(*b*)

Figure 2
(*a*) Three-dimensional deformation electron-density map as rapidly obtained from fast Fourier transform by the program *molecoolQt* (Hübschle & Dittrich, 2011) with turquoise/orange isosurfaces of ±0.056 e Å^{-3}. The molecular dipole moment vector from invariom refinement (red color) is compared with the theoretical DFT result (green, see text), both with a scale of 0.5 Debye per Å. (*b*) Electrostatic potential of ceftazidime mapped on the 0.0067 e Å^{-3} electron-density isosurface.

[1] Supplementary data for this paper are available from the IUCr electronic archives (Reference: GW5017). Services for accessing these data are described at the back of the journal.

calculated from the database parameters do not correspond to a polarized molecule perturbed by crystal packing and hydrogen bonding, but to an idealized molecule in the gas phase with the conformation found in the crystal. Hence, the influence of the water solvent on the molecular electron density cannot be studied experimentally without high-resolution data. However, considering the limitations of the IAM, taking into account atomic charges and aspherical valence electron density by scattering-factor databases is certainly an important improvement, and derived properties do not require time-consuming quantum mechanical calculations.

As pointed out by Spackman (1992), the molecular dipole moment is a 'compact summary of the molecular charge distribution'. We therefore consider it to be of importance with respect to the comparison of a series of pharmaceutically active molecules. In ceftadizime the value is 21.8 Debye, with an x component of 1.1, a y component of 20.6 and a z component of −7.1. The direction of the dipole-moment vector is shown as originating from the center of mass of the molecule in Fig. 2(*a*) (generated by *molecoolQt*) with a scale of 0.5 Å per Debye in red color. The dipole moment is dominated by the opposite charges of the pyridinum and the carboxylate groups. This explains its large magnitude. A benchmark value is provided by a single-point energy calculation using the same molecular orientation and geometry [method/basis set choice: B3LYP/D95++(3df,3pd)], which yields comparable results to summing up the contributions of aspherical-atom density fragments: the DFT dipole moment is 15.1 Debye, with $x = -0.05$, $y = 14.90$ and $z = -2.33$. The theoretical result is included in Fig. 2(*a*) as a vector in green. We have noted on several occasions that dipole moments generated from the invariom database can anticipate a part of the in-crystal enhancement when compared with the isolated molecular result. This could be due to the approximation of reproducing molecular electron density from fragments derived from model compounds. Furthermore, systematic comparisons between *ab initio* dipole moments and the result after multipole projection have shown that the dipole moment for sulfur containing compounds is not as well reproduced as for compounds containing the elements C, H, N and O. Choices in the database generation process like *e.g.* refining or not refining the scale factor can change the invariom dipole magnitude by 5% for ceftazidime – while not significantly altering the fit to the experimetal data. Such changes illustrate that the Hansen–Coppens multipole model has a limited accuracy in reproducing dipole moments from more sophisticated theoretical calculations. Nevertheless, directions of both vectors shown in Fig. 2(*a*) agree fairly well with 11.04° and the accuracy reached is acceptable for high-throughput screening.

Molecular electrostatics have been used for decades in drug design, since they provide a simplified yet accurate means to understand the drug–receptor interaction process (Náray-Szabó & Ferenczy, 1995). Fig. 2(*b*) shows the molecular electrostatic potential (ESP) of ceftazidime with water molecules omitted. To illustrate the distribution of positive and negative values, this property is color-coded on an isosurface of molecular electron density with a value of 0.0067 e Å^{-3}, corresponding to 0.001 a.u. This value has been recommended by Politzer *et al.* (2001). Since ceftazidime molecules are zwitterionic in the pentahydrate structure, the minimum and maximum values of the potential are comparably large. A feature common to all β-lactam antibiotics is a strongly negative region of the carboxylate group that extends to the neighboring β-lactam oxygen (Wagner *et al.*, 2004). We plan to compare several cephalosporin antibiotics in the future to see if the similarities in the electrostatic potential that we found for the fluoroquinolone class of antibiotics (Holstein *et al.*, 2012) – for those configurations sharing the same ionization state – are also present in several cephalosporin molecules. Since molecular flexibility and dimensions can be quite different for cephalosporins we consider the question of similarity of the molecular ESP to be of high relevance.

4. Conclusion

Requirements for using charge-density methodology as a tool in high-throughput screening are fulfilled today. Single-crystal X-ray diffraction can indeed be used as a technique for screening hundreds of compounds in a short amount of time when single crystals are available. Crystallization is the remaining bottleneck, and so are other aspects of the experimental procedure like specimen selection and data reduction, which might be hard to automate and may now require more time than data collection/refinement itself. Invarioms provide a model of the aspherical electron-density and allow to extract more information from a standard single-crystal diffraction experiment. Invariom modeling is automated and rapid; disordered structures still require manual intervention and checking. Properties that can be screened are bond-topological parameters, empirical hydrogen-bond energies, electrostatic potentials and the molecular dipole moment. These can all be derived at low computational cost with an acceptable accuracy.

Funding from the Deutsche Forschungsgemeinschaft DFG for an Emmy Noether research fellowship, DI 921/3–2, is gratefully acknowledged. We also thank S. Becker (MPI), T. Grüne and G. M. Sheldrick (program xds2sad) for support and S. Siemsen for corrections in the manuscript.

References

Bader, R. F. W. (1990). *Atoms in Molecules: A Quantum Theory*. Oxford: Clarendon Press.
Blessing, R. H. (1995). *Acta Cryst.* A**51**, 33–38.
Broennimann, Ch., Eikenberry, E. F., Henrich, B., Horisberger, R., Huelsen, G., Pohl, E., Schmitt, B., Schulze-Briese, C., Suzuki, M., Tomizaki, T., Toyokawa, H. & Wagner, A. (2006). *J. Synchrotron Rad.* **13**, 120–130.
Bronnimann, C., Eikenberry, E. F., Horisberger, R., Hulsen, G., Schmitt, B., Schulze-Briese, C. & Tomizaki, T. (2003). *Nucl. Instrum. Methods Phys. Rev. A*, **510**, 24–28.
Burnett, M. N. & Johnson, C. K. (1996). *ORTEP*III. Technical Report ORNL-6895. Oak Ridge National Laboratory, Tennessee, USA.
Coppens, P., Sabine, T. M., Delaplane, G. & Ibers, J. A. (1969). *Acta Cryst.* B**25**, 2451–2458.
Dittrich, B., Hübschle, C. B., Luger, P. & Spackman, M. A. (2006). *Acta Cryst.* D**62**, 1325–1335.
Dittrich, B., Hübschle, C. B., Messerschmidt, M., Kalinowski, R., Girnt, D. & Luger, P. (2005). *Acta Cryst.* A**61**, 314–320.
Dittrich, B., Koritsánszky, T. & Luger, P. (2004). *Angew. Chem. Int. Ed.* **43**, 2718–2721.
Dittrich, B., Strumpel, M., Schäfer, M., Spackman, M. A. & Koritsánszky, T. (2006). *Acta Cryst.* A**62**, 217–223.
Dominiak, P. M., Volkov, A., Li, X., Messerschmidt, M. & Coppens, P. (2007). *J. Chem. Theory Comput.* **2**, 232–247.
Espinosa, E., Molins, E. & Lecomte, C. (1998). *Chem. Phys. Lett.* **285**, 170–173.
Flack, H. D. (1983). *Acta Cryst.* A**39**, 876–881.
Hansen, N. K. & Coppens, P. (1978). *Acta Cryst.* A**34**, 909–921.
Hirshfeld, F. L. (1976). *Acta Cryst.* A**32**, 239–244.
Holstein, J. J., Hübschle, C. B. & Dittrich, B. (2012). *CrystEngComm*, **14**, 2520–2531.
Hübschle, C. B. & Dittrich, B. (2011). *J. Appl. Cryst.* **44**, 238–240.
Hübschle, C. B., Luger, P. & Dittrich, B. (2007). *J. Appl. Cryst.* **40**, 623–627.
Hübschle, C. B., Sheldrick, G. M. & Dittrich, B. (2011). *J. Appl. Cryst.* **44**, 1281–1284.
Iversen, B. B., Larsen, F. K., Pinkerton, A. A., Martin, A., Darovsky, A. & Reynolds, P. A. (1999). *Acta Cryst.* B**55**, 363–374.
Kabsch, W. (2010). *Acta Cryst.* D**66**, 125–132.
Kemperman, G. J., de Gelder, R., Dommerholt, F. J., Raemakers-Franken, P. C., Klunder, A. J. H. & Zwanenburg, B. (1999). *Chem. Eur. J.* **5**, 2163–2168.

Kemperman, G. J., de Gelder, R., Dommerholt, F. J., Raemakers-Franken, P. C., Klunder, A. J. H. & Zwanenburg, B. (2000). *J. Chem. Soc. Perkin Trans. 2*, pp. 1425–1429.
Kemperman, G. J., de Gelder, R., Dommerholt, F. J., Raemakers-Franken, P. C., Klunder, A. J. H. & Zwanenburg, B. (2001). *Eur. J. Org. Chem.* pp. 3641–3650.
Kennedy, A. R., Okoth, M. O., Sheen, D. B., Sherwood, J. N., Teat, S. J. & Vrcelj, R. M. (2003). *Acta Cryst.* C**59**, o650–o652.
Koritsanszky, T., Flaig, R., Zobel, D., Krane, H., Morgenroth, W. & Luger, P. (1998). *Science*, **279**, 356–358.
Koritsánszky, T., Richter, T., Macchi, P., Volkov, A., Gatti, C., Howard, S., Mallinson, P. R., Farrugia, L., Su, Z. W. & Hansen, N. K. (2003). *XD*. Technical Report. Freie Universität Berlin, Germany.
Luger, P. (2007). *Org. Biomol. Chem.* **5**, 2529–2540.
Luger, P., Wagner, A., Hübschle, C. B. & Troyanov, S. I. (2005). *J. Phys. Chem. A*, **109**, 10177–10179.
Macchi, P., Proserpio, D. M., Sironi, A., Soave, R. & Destro, R. (1998). *J. Appl. Cryst.* **31**, 583–588.
Náray-Szabó, G. & Ferenczy, G. G. (1995). *Chem. Rev.* **95**, 829–847.
Politzer, P., Murray, J. S. & Preralta-Inga, Z. (2001). *Int. J. Quant. Chem.* **85**, 676–684.
Powers, R. A., Caselli, E., Focia, P. J., Prati, F. & Shoichet, B. K. (2001). *Biochem.* **40**, 9207–9214.
Sheldrick, G. M. (2008*a*). *Acta Cryst.* A**64**, 112–122.
Sheldrick, G. M. (2008*b*). *SADABS*, Version 2008/1. University of Göttingen, Germany.
Spackman, M. A. (1992). *Chem. Rev.* **92**, 1769–1797.
Spackman, M. A., Munshi, P. & Dittrich, B. (2007). *ChemPhysChem*, **8**, 2051–2063.
Spek, A. L. (2009). *Acta Cryst.* D**65**, 148–155.
Stephenson, G. A. & Diseroad, B. A. (2000). *Int. J. Pharm.* **198**, 167–177.
Su, Z. & Coppens, P. (1992). *Acta Cryst.* A**48**, 188–197.
Toyokawa, H., Broennimann, C., Eikenberry, E., Henrich, B., Kawase, M., Kobas, M., Kraft, P., Sato, M., Schmitt, B., Suzuki, M., Tanida, H. & Uruga, T. (2010). *Nucl. Instrum. Methods Phys. Res. A*, **623**, 204–206.
Volkov, A., Macchi, P., Farrugia, L. J., Gatti, C., Mallinson, P., Richter, T. & Koritsánszky, T. (2006). *XD*2006. University at Buffalo, State University of New York, NY, USA; University of Milano, Italy; University of Glasgow, UK; CNRISTM, Milano, Italy; Middle Tennessee State University, TN, USA.
Wagner, A., Flaig, R., Dittrich, B., Schmidt, H., Koritsánszky, T. & Luger, P. (2004). *Chem. Eur. J.* **10**, 2977–2982.
Zarychta, B., Pichon-Pesme, V., Guillot, B., Lecomte, C. & Jelsch, C. (2007). *Acta Cryst.* A**63**, 108–125.